

A NOVEL ALGORITHM TO REDUCE PEAK-TO-AVERAGE POWER RATIO OF ORTHOGONAL FREQUENCY DIVISION MULTIPLEXING SIGNALS

¹ MANZOOR AHMED HASHMANI, ² FARZANA RAUF ABRO, ³ MUKHTIAR ALI UNAR,
⁴ JUNZO WATADA

¹ Associate Professor, University Technology Petronas, High Performance Cloud Computing Center (HPC3),
Department of Computer and Information Sciences, Malaysia

² Associate Professor, Mehran University of Engineering and Technology, Department of Electronic
Engineering, Pakistan

³ Professor, Mehran University of Engineering and Technology, Department of Computer Systems
Engineering, Pakistan

⁴ Professor, University Technology Petronas, Department of Computer and Information Sciences, Malaysia

E-mail: ¹manzoor.hashmani@utp.edu.my; mhashmani@yahoo.com, ²far786_abro@yahoo.com,
³mukhtiar.unar@faculty.muett.edu.pk, ⁴junzo.watada@utp.edu.my

ABSTRACT

It has been observed over last several decades that bandwidth greediness of applications never gets fulfilled. Hence, scientists, researchers, and engineers keep working on new ways of providing higher bandwidth. Recently, a new modulation technique called Orthogonal Frequency Division Multiplexing (OFDM) has been introduced which provides very high data rates. In OFDM the high frequency input signal is modulated over a large number of low frequency sub-carrier signals which are orthogonal to each other. This feature makes it very robust against efficiency degradation at higher frequencies. That is the reason why OFDM is a choice for the modern high and ultra-high data rate communication systems. However, it suffers from high levels of the peak power to the average power also called Peak-to-Average Power Ratio or PAPR. Reducing PAPR in OFDM is a hot research area. There are many schemes available which attempt to reduce PAPR. Some are in fact able to reduce PAPR but not sufficient enough to make these feasible. Others do reduce it but increase its complexity to an extent that these become unfeasible to realize. From literature it has been identified that SLM performs better than other methods in terms of computational complexity at the same performance level.

The main motivation behind this research effort is to find a mechanism which reduces PAPR for OFDM systems and has a reasonable level of complexity so that it may be realizable. As an outcome of this research activity, a novel framework based on Artificial Neural Networks (ANN) and Selective Mapping (SLM) is proposed. The kernel used by the ANN in proposed framework is a modified version (proposed by us) of an already available kernel called Novel Kernel Based – Radial Basis Function (NKB-RBF). We show through simulations results that our proposed kernel, Modified NKB-RBF (MNKB-RBF), is more efficient than NKB-RBF and gives better results in selection of low frequency sub-carriers with lowest PAPR.

Keywords: Orthogonal Frequency Division Multiplexing (OFDM), Peak-to-Average Power Ratio (PAPR), Selective Mapping (SLM), Artificial Neural Networks (ANN), Radial Basis Function (RBF)

1. INTRODUCTION

As the data rates of communication systems increase so does the demand by the applications. Current applications, like high definition TV, good quality video, on-line gaming, vehicle navigation systems, etc., demand ultra-high data rates. Another demand of modern applications is an ability of the communication systems to sustain these high data rates without service disruption, for example, to devices present in vehicles moving at very high speed, i.e., fast moving cars, electric trains, airplanes, etc. These demands of high data rates with seamless service require new and ingenious techniques to be employed in communication systems. In order to fulfil this requirement, one area of focus is the modulation techniques because efficient modulation techniques can multiply the data rates.

Recently, a new modulation technique called Orthogonal Frequency Division Multiplexing (OFDM) has been introduced which provides very high data rates and is based on multiplexing of frequencies [1]. The key feature of OFDM is the orthogonality of carrier frequencies. This feature makes it very robust against efficiency degradation at higher frequencies unlike other modulation techniques which suffer from substantial degradation of service at higher frequencies. This is the reason for the OFDM to be a choice technology for the modern high and ultra-high data rate communication systems [2].

However, OFDM suffers from high levels of the peak power to the average power ratio also called Peak-to-Average Power Ratio (PAPR). In OFDM, PAPR is high mainly due to the reason that the summation of peaks of many sub-carriers may result in very high value. Note that in OFDM the high frequency input signal is modulated over a large number of low frequency sub-carrier signals which are orthogonal to each other. Though the average of these sub-carriers would be quite low, the peak power which is the summation of all peaks may become very high.

Reducing PAPR in OFDM is a hot research area. There are many schemes available which attempt to reduce PAPR. Some are in fact able to reduce PAPR but not sufficient enough to make these feasible. Others do reduce it but increase its complexity to an extent that these become unfeasible to realize. Sufficient details of these schemes, their merits and demerits are provided in literature. However, the issue is not settled yet.

The rest of the paper is organized as follows. In section 2, we visit basics of OFDM and the importance of PAPR to refresh the knowhow of the reader. In section 3, we list and elaborate upon various well-known and promising PAPR reduction schemes. The information presented in this section is obtained through the survey of the available literature on the subject matter. In particular, we show in this section that SLM, one of these scheme, has better promise to reduce PAPR along with an issue that is a major bottleneck in its performance. In section 4, we propose a modified RBF kernel called MNKB-RBF which is going to be the main component of our proposed PAPR reduction scheme as detailed in section 5. In section 6, we present the evaluation of our proposed scheme and establish that it performs better. And finally, we conclude this paper in section 7.

2. OFDM & PAPR

2.1 OFDM

OFDM is a modulation technique which uses multiple low frequency sub-carriers (orthogonal to each other) instead of a single high frequency carrier and is very popular these days to transmit high speed digital data [3][6]. Since, each sub-carrier is of low frequency, modulation is done at low symbol rate. However, overall symbol rate is quite high because multiple sub-carriers are used.

We know that using high symbol rate over a single carrier results in severe channel conditions (attenuation, interference, fading, etc.). In OFDM, these conditions are reduced substantially due to low symbol rate on each sub-carrier. Moreover, due to low symbol rate we do not need to use a guard interval between symbols. This results in elimination of Inter-Symbol Interference (ISI) and achievement of better Signal-to-Noise Ratio (SNR).

2.2 PAPR

In OFDM System Model, the input channel signals are modulated first using either Phase Shift Keying (PSK) or Quadrature Amplitude Modulation (QAM) and then undergo Inverse Fast Fourier Transform (IFFT) operation at the transmitter end [7][8]. This creates low-frequency sub-carriers (orthogonal to one another) at the transmitter side [9]. These transmitted signals can deliver high peak values in the time domain and these high peak values when get summed up due to alignment produce high ratio of peak power to the average power [4]. The high PAPR is a

consequence of the summing up of sonic waves and non-constant envelope [10]. The injurious effect of high PAPR is that it brings down the performance of power amplifier. Therefore, RF power amplifiers need to be controlled in a very large linear region, otherwise the signal peaks will enter into a non-linear region and will cause deformation. Though there are many schemes which reduce PAPR, the efficiency of any PAPR reduction scheme is measured through Cumulative Distribution Function (CDF) [5]. PAPR of a signal is calculated using equation (1) [11]. Here, $E[\cdot]$ indicates the Expectation Operator.

$$PAPR(x) = \frac{\max |x(t)|^2}{E[|x(t)|^2]} \quad (1)$$

2.3 Research Motivation

In today's digital world, the explosive usage of Big Data, Internet of Things, real-time multimedia streaming, etc. demand efficient mechanisms to seamlessly accommodate massive wireless data transmissions. The 4th generation communication systems use OFDM as a high-data rate multiplexing agent to transmit large data at higher data rates. However, the highest data rate that can be accommodated by the OFDM is limited by the well-known PAPR problem. Therefore, it is pertinent and need of the hour to solve PAPR problem in order for the OFDM to be used by the 4th and 5th generation wireless communication systems at still higher data rates. In this paper, we propose a mechanism to maximize the bandwidth utilization in OFDM by using PAPR minimization. This mechanism is expected to act as major contribution for 5th generation communication systems as well.

2.4 Research Objectives

The objectives of this research are;

- Investigate the existing techniques which give better results in selection of low frequency sub-carriers with low PAPR.
- Find mechanism to reduce the PAPR of OFDM systems with less complexity to utilize the maximum bandwidth of OFDM.

3. PAPR REDUCTION SCHEMES – A LITERATURE SURVEY

This section describes various PAPR reduction schemes and discusses their performance as given in the literature. The performance comparison in

tabular form is shown in Table 1. In [12], it has been shown that Selective Mapping is a better candidate for potential to reduce PAPR and remains computational less complex.

Table 1: Performance of PAPR Reduction Techniques

S#	Technique	Performance
1.	Selective Mapping	<ul style="list-style-type: none"> • Reduces Distortion • No Power Raise • Selects lowest PAPR sub-carriers
2.	Partial Transmit Sequence	<ul style="list-style-type: none"> • Reduces Distortion • No Power Raise • High Computational Complexity
3.	Tone Reservation	<ul style="list-style-type: none"> • Reduces Distortion • Power Gets Raised • Less Complex than PTS
4.	Tone Injection	<ul style="list-style-type: none"> • Reduces Distortion • Power Gets Raised • PAPR Reduction without Data Rate Reduction
5.	Clipping and Filtering	<ul style="list-style-type: none"> • Introduces Distortion • No Power Raise • One of the Simplest

3.1 Selective Mapping

The research that introduced the “Selective Mapping Technique” was penned down by Bamul, Fischer and Huber in 1996 [13]. SLM is one of the most favorable PAPR reduction techniques as it does not introduce distortion and effectively reduces PAPR [12][13][14][15]. In this technique the input data blocks are multiplied by each of the given phase-rotated sequences to generate alternative input symbol sequences. Part of the alternative sequences is processed further under IFFT and their PAPR is determined. Then the signal with lowest PAPR is selected for transmission [13][14][15].

In SLM, input data is partitioned into smaller data blocks which result in parallel data streams. Each element in a data block is multiplied by a phase-rotated sequence [13][14][15].

The fundamental idea that lies in this technique is that it helps to select the signal with lowest PAPR value from a pool of phase-rotated sequences.

3.2 Issue of SLM Scheme

SLM scheme is based on the core principle of selecting one sequence of sub-carriers (lowest PAPR) from a set of available sequences of phase-rotated sub-carriers. Selection of a particular sequence is a major issue and determines the

performance of SLM in terms of the magnitude by which the PAPR is reduced. Selection of an appropriate phase-rotated sequence of sub-carriers is essentially an optimization problem. We intend to solve the above stated problem by using the ANN (Artificial Neural Networks) framework. ANN is one of the best ways to solve optimization problems.

4. PROPOSAL OF MODIFIED NKB-RBF

4.1 Artificial Neural Networks and Radial Basis Functions

Computational model for ANNs was first proposed by McCulloch and Pitts [16]. Since then, ANNs have been recognized as a decision making tool by many researches [17][18]. ANN are particularly very useful in solving optimization problems. An optimization problem is either difficult or almost impossible to solve with the help of conventional rule-based programming [19].

An RBF network [20] is an ANN whose activation functions are radial basis functions. It

was first introduced by Broomead and Lowe [21] and since then it has become a very popular methodology to solve optimization problems that suit ANN paradigm [19][20][21]. The main advantage of RBF when compared with other algorithms based on ANN paradigms is the simplicity of the computation of network parameters [20]. RBF networks have been used in diverse optimization domains, including pattern classification [22], time series prediction [23], systems and control [24], and function approximation [25].

In the conventional RBF kernel, mostly Gaussian of the Euclidean distance between feature vector and neuron's center is used [26]. However, there can be scenarios where Euclidean distance is not the dominant measure to find separation among the features, for example, if two feature vectors are separated by equal distance from the center but separated from the center via unequal angles. In that case, the cosine of the angle can play a vital role in differentiating the feature vectors.

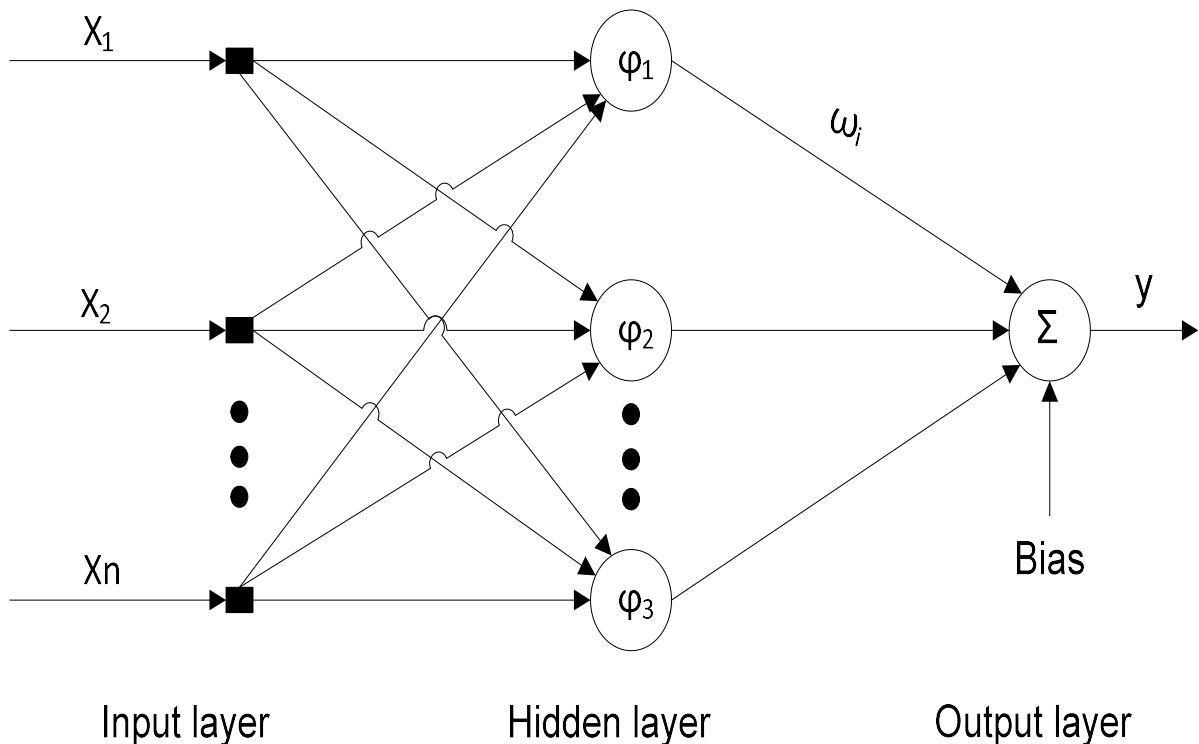


Figure 1: Architecture of the RBF Based ANN

4.2 Conventional RBF

RBF networks in their general form consist of three layers. These layers are called an input layer, a hidden layer, and a linear output layer. The hidden layer is one where nonlinear activation functions operate. The layout is shown in Figure 1. Generally, the input is a real vector, $x \in R^n$. The network output maps the input vector to a scalar, $y: R^n \rightarrow R$, which is achieved using equation (2).

$$y_j = \sum_{i=1}^N \omega_i \varphi_i(\|x - c_i\|) + b_j \quad \forall j = 1, 2, \dots, N_o \quad (2)$$

Where N and N_o are the number of hidden and output layer neurons, respectively, $c_i \in R^n$ is the center for i^{th} neuron, ω_i is output layer weight for i^{th} neuron, b_j is the bias term for the j^{th} output neuron, and φ_i is the basis function associated with i^{th} hidden neuron.

The domain of activation function is typically taken to be the Euclidean distance between input and the centers of every neuron. Most commonly used RBF kernels are multi-quadrics, inverse multi-quadrics and Gaussian.

4.3 Recently Proposed “Novel Kernel Based RBF (NKB-RBF)”

Motivated by the observation that “in many scenarios Euclidean distance (ED) is not the dominant measure to find the separation among features”, Aftab et.al, propose in [27] a novel RBF kernel which consists of a linear combination of Gaussian and cosine RBF kernels. The cosine RBF kernel computes the cosine of the angle between supplied feature vector and the center vector associated with that neuron.

Aftab et.al, in [27] state that intuition suggests that ED is not the only measure to contrast the FVs. For example, in the case when FVs are equally separated in distance, then the ED will be no more effective. To deal with this issue, they proposed a generalized RBF kernel by linearly combining the conventional ED based RBF kernel and a cosine based RBF kernel which is formulated as given in equation (3).

$$\varphi_i(x, c_i) = \alpha_1 \varphi_{i1}(x, c_i) + \alpha_2 \varphi_{i2}(\|x - c_i\|) \quad (3)$$

Where α_1, α_2 are weightage parameters for cosine and Euclidean kernels, respectively, which can acquire values in this range: $0 \leq \alpha_1, \alpha_2 \leq 1$.

4.4 Issues of NKB-RBF

Recently proposed Novel Kernel Based RBF (NKB-RBF) is shown in [27] to perform well with different problems as it utilizes the complimentary property of two kernels that are based on the Euclidean (distance) and Cosine (angle) or correlation measure. However, the NKB-RBF suffers from the manual selection of the mixing parameter.

We can see in equation (2) that α_1 and α_2 are the mixing parameters of Cosine and Euclidean kernels. The manual selection (as suggested by MNKB-RBF) of the mixing parameters α_1 and α_2 is a critical issue particularly in the situations with no generalization of the problem. For the selection of these mixing parameters one needs prior information about the problem. In cases where cosine is the good measure of similarity or in other words the angle is the discriminating element we will have to choose higher value for α_1 (close to 1) and lower value for α_2 (close to 0) to have optimal performance. The reverse must be selected for these mixing parameters, i.e., α_1 (close to 0) and higher value for α_2 (close to 1), for the problem where angle is not the optimal discriminating element. If this guide line is not followed, we will face degradation in performance instead of improvement. Table 2 shows the criteria for the manual selection of mixing parameters α_1 and α_2 .

Table 2: Criteria for Manual Selection of Parameters α_1 and α_2

α_1	α_2
<ul style="list-style-type: none"> • Weightage to the Cosine Distance (CD) should be high in case where CD is the distinguishing element. • Should be low if the CD is the confusion factor. • NKB-RBF allows to choose α_1 manually which is not possible in the dynamic scenario of SLM 	<ul style="list-style-type: none"> • Weightage to the Euclidean Distance (ED) should be high in case where ED is the distinguishing element. • Should be low if the ED is the confusion factor. • NKB-RBF allows to choose α_2 manually which is not possible in the dynamic scenario of SLM

To get the best performance from the NKB-RBF one needs to select the optimal values of the mixing parameters. The manual selection of mixing parameters as suggested by NKB-RBF requires prior knowledge of the system. This restricts the application of NKB-RBF to only the problems where prior information about the system is known. In the case of SLM, we need as adaptive optimization algorithm that can select the optimal weights of the individual kernels to harness the complimentary properties of the two kernels without the prior knowledge of the incoming signal type.

4.5 Proposed Solution: Modified NKB-RBF (MNKB-RBF)

The critical issue of NKB-RBF is the manual tuning of the mixing parameters α_1 and α_2 . In order to use it for optimization of selection of one phase rotated sub-sequence of signals among many candidate in SLM (with minimum PAPR), we need to make the tuning of α_1 and α_2 dynamically adaptive. Since the core objective of the proposed adaptive algorithm is to minimize the overall error of the system, we propose to use the error energy besides distance for tuning of α_1 and α_2 . We call our new algorithm as Modified NKB-RBF or MNKB-RBF in short.

In order to incorporate the error energy, we replace α_1 and α_2 with the $\eta(n)$ and $1-\eta(n)$ in equation (3), to make them time varying as shown in equation (4). We can rewrite the kernel equation as:

$$\varphi_i(x, c_i) = \eta(n)\varphi_{i1}(x, c_i) + (1 - \eta(n))\varphi_{i2}(\|x - c_i\|) \quad (4)$$

Where,

- $\eta(n)$ = weight of Cosine Distance (CD)
- $1 - \eta(n)$ = weight of Euclidean Distance (ED)

The MNKB-RBF algorithm uses the update rule of a Robust Variable Step-Size Least Mean Square (RVS-SLMS) algorithm [28] for its learning rate where the update is obtained by an estimate of the autocorrelation between current error $e(n)$ and past error $e(n-1)$.

If $\rho(n)$ is the final output error, the error energy of the MNKB-RBF algorithm is defined as follows:

$$\rho(n) = \beta \rho(n) + (1 - \beta)e(n)e(n - 1) \quad \text{where } 0 < \beta < 1$$

Note that $\rho(n)$ is the error energy at n^{th} instant.

In the proposed method the weight of the cosine kernel can be calculated as follows:

$$\eta(n + 1) = \tau * \eta(n) + \sigma \rho(n) \quad \text{where } 0 < \tau < 1, 0 < \sigma < 1$$

Here $\eta(n+1)$ is the weight of the Cosine Distance for next iteration and τ , σ and β are the momentum coefficients.

$$\eta(n + 1) = \begin{cases} 1, & \eta(n + 1) > 1 \\ \eta(n + 1), & 0 < \eta(n + 1) < 1 \\ 0, & \eta(n + 1) < 0 \end{cases}$$

MNKB-RBF based SLM Module

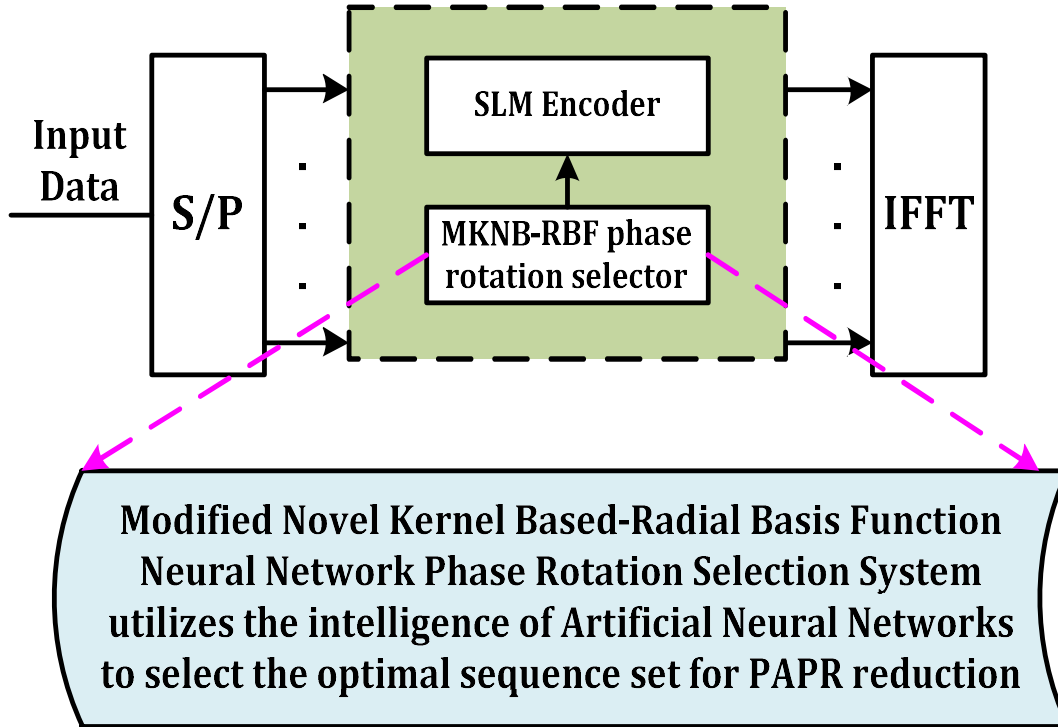


Figure 2: Block Diagram of the Proposed PAPR Reduction Scheme using MNKB-RBF

5 PROPOSAL OF A NOVEL PAPR REDUCTION SCHEME BASED ON MNKB-RBF

In previous, we proposed a novel technique for the autonomous selection of weights of mixing parameters of the NKB-RBF algorithm and named it MNKB-RBF. The proposed kernel can be used in the dynamic environments where little or no prior information about the discriminating measure is known. As in the case of Selective Mapping (SLM) we want to make our system adaptive and suitable for dynamically selecting an optimal sub-sequence (with lowest PAPR) from a set of available sub-sequences of the frequencies with unknown effects on PAPR. The proposed kernel is expected to perform well in this scenario because it autonomously selects weights based on the error energy.

Framework of proposed technique (based on MNKB-RBF and SLM) is shown in Figure 2, which selects the sub-sequence with the lowest PAPR from the given sequences. From this figure it can be seen that the selection of the optimal phase

rotation is performed by advanced technique of optimized weighted kernel. In the proposed system the signal will first pass through the frequency transformation block and then the SLM block, which will select the appropriate carrier signal for the given signal.

The SLM block is modified to indicate the selection of the best carrier sub-sequence based on the intelligent decision of the dynamic method of MNKB-RBF to minimize the chances of the rise in PAPR. The argument is supported by extensive simulations/experiments performed and discussed in next section.

6 PERFORMANCE EVALUATION OF PROPOSED PAPR REDUCTION SCHEME

The performance of the proposed scheme for selection of a phase-rotated sequence of signals from a set of available sequences depends on MNKB-RBF and SLM (Selective Mapping). Since SLM is already a known and evaluated scheme,

hence the performance of our scheme solely depends upon the performance of MNKB-RBF. In this section, a thorough evaluation of our scheme is presented and we show that it performs better than the scheme which uses SLM and NKB-RBF.

6.1 Performance Evaluation Environment

We have performed a comprehensive evaluation of MNKB-RBF (Modified Novel Kernel Based RBF) against NKB-RBF (Novel Kernel Based RBF) by using simulations of ANNs on MATLAB using these kernels.

In order to have a good level of confidence in the deductions that we make after comparison of these two kernels, nine different datasets have been generated on which the performances of both of these kernels are tested and compared. The details of the simulation environment, test cases, and the nature of the datasets are being given in the following section.

In order to compute final output error $\rho(n)$ and error energy of the MNKB-RBF algorithm we used following variables:

- CD – Cosine Distance
- ED – Euclidean Distance
- $\alpha_1 \alpha_2$ – Mixing Parameters
- ϕ – Error Energy
- $e(n)$ – Current Error
- $e(n-1)$ – Past Error

6.2 Simulation Environment & Test Cases

In order to train and test the ANNs which use the Novel RBF and the proposed RBF (MNKB-RBF), first of all nine different datasets of one hundred randomly generated messages are generated. In each dataset, the initial fifty messages are for the purpose of training the ANN and the later fifty messages are to be used for testing the performance of the ANN.

6.2.1 Regarding Datasets

Regarding dataset 1, 2, and 3, the carrier is to be selected from a pool of 64 sequences of phase-rotated carriers. However, 8-QAM (Quadrature Amplitude Modulation), 16-QAM, and 32-QAM are used to modulate each message in dataset 1, dataset 2, and dataset 3 respectively. This is done in order to see whether or not changing modulation changes the pattern of results or leads to the same conclusion. In our graphic or numeric results are indicated the nature of dataset by the following scheme [64 x 8], [64 x 16] and [64 x 32]. In this

scheme, the first numeric value indicates the number of phase-rotated sequences in the pool and the second numeric value represents the number of symbols used in QAM for modulation, for example, in [64 x 8], the pool has 64 sequences and 8 symbols are used to modulate the messages.

Similarly, in dataset 4, 5, and 6, the pool has 128 phase-rotated sequences with messages modulated using 8-QAM, 16-QAM, and 32-QAM respectively.

Lastly, in dataset 7, 8, and 9, there are 256 phase rotated sequences and messages are modulated using 8-QAM, 16-QAM, and 32-QAM respectively.

6.2.2 Regarding Test Cases

Multiple iterations of simulations are performed for both “Training Phase” as well as “Testing Phase” on all of the datasets as specified in the above section. Large number of iterations are performed to enhance the reliability of the deductions.

6.3 Training Results

Training of both kernels, i.e., NKB-RBF and MNKB-RBF is done using three different training cases. Each test case consists of tests done on three datasets of similar nature as listed below.

Training Case I: Dataset having 64 phase-rotated sequences.

- Dataset 1 – [64 x 8]
- Dataset 2 – [64 x 16]
- Dataset 3 – [64 x 32]

Training Case II: 128 sequences

- Dataset 4 – [128 x 8]
- Dataset 5 – [128 x 16]
- Dataset 6 – [128 x 32]

Training Case III: 256 sequences

- Dataset 7 – [256 x 8]
- Dataset 8 – [256 x 16]
- Dataset 9 – [256 x 32]

The results of the training phase in graphical form are shown in Figures 3 to Figure 11. The results correspond to Training Case I, Training Case II and Training Case III respectively. Evaluation and analysis of training phase results are given in the next section.

6.3.1 Evaluation, Analysis, and Deductions

The x-axis in these graphs (Figures 3 to 11) represent the number of epochs for which the simulation was run. The y-axis gives the magnitude of the mean of the squared error (MSE). Each graph has two curves, i.e., the dashed-line curve (red colored curve) for the Novel RBF (NKB-RBF) and the solid-line curve (blue curve) for the Proposed RBF (MNKB-RBF).

Let us first of all analyze graphs of the “Training Case I” (64 sequences of carriers) in Figure 3. It can be seen that 8 symbols are used for modulation and that for only the first epoch, the MSE (Mean Square Error) is higher for MNKB-RBF. Whereas, from 2nd epoch and onwards, MSE for MNKB-RBF is lower than NKB-RBF. This indicates much early successful training of ANN which uses our proposed kernel. After around only 7th epoch, MSE for MNKB-RBF reaches its minimum which is 2 and is an excellent result showing that less time is needed to train MNKB-RBF based ANN.

It can be also seen that curves in Figure 4 & Figure 5 do not show substantial change in their pattern even after increase in modulation symbols from 8 to 16 and 32. **This leads us to deduce that MNKB-RBF is robust against variation in modulation symbol rate.** This is important for MNKB-RBF to be indeed practically used in not only PAPR reduction schemes but also in other optimization applications.

Let us now focus on results of “Training Case II & III” which are shown in Figures 6 to Figure 11. Some interesting observations can be made. For one, the performance of MNKB-RBF

does not change even though the pool of candidate phase-rotated sequences is increased from 64 to 256. In all of these graphs it can be seen that MSE exponentially reduces (solid blue curve) and minimizes after around 7 epochs. **This analysis leads us to the deduction that MNKB-RBF is robust against variation in the size of the pool of phase-rotated carrier sequences as well.**

On the other hand, the performance of NKB-RBF has degraded with increase in the pool size of carrier sequences. MSE for NKB-RBF is not reducing fast enough which is evident from the less steepness of the dashed-line red curves for NKB-RBF in Figure 3 to Figure 11.

Now look at the final value of MSE for which both NKB-RBF and MNKB-RBF stabilize. It is visible in these graphs that the final MSE value for NKB-RBF is around 5, whereas **for MNKB-RBF, MSE keeps on decreasing as we increase the size of the pool of sequences and becomes almost zero.** We have summarized the final MSE values (approximated) against size of pool of sequences in the following table for MNKB-RBF. Hence, **we conclude that MNKB-RBF performs much better than NKB-RBF in terms of training of ANN.**

Table 3: Final Mean Square Error (MSE) Comparison

Size of Pool of Carrier Sequences	MSE for Novel RBF	MSE for Proposed RBF
64	4.0	2.0
128	3.5	1.0
256	3.0	0.1

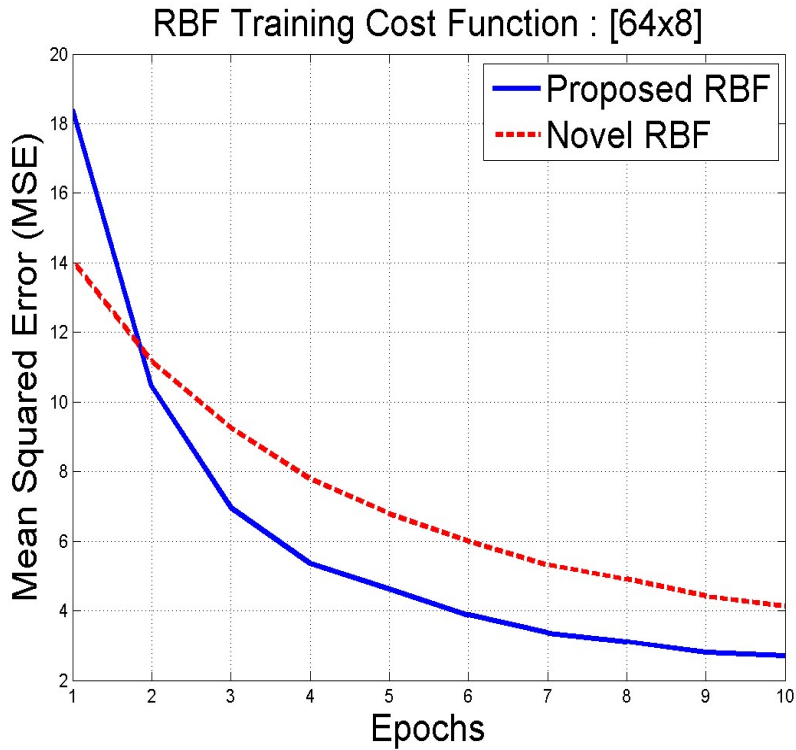


Figure 3: Training cost comparison between Novel RBF and Proposed RBF (Sequences = 64, Modulation = 8-QAM)

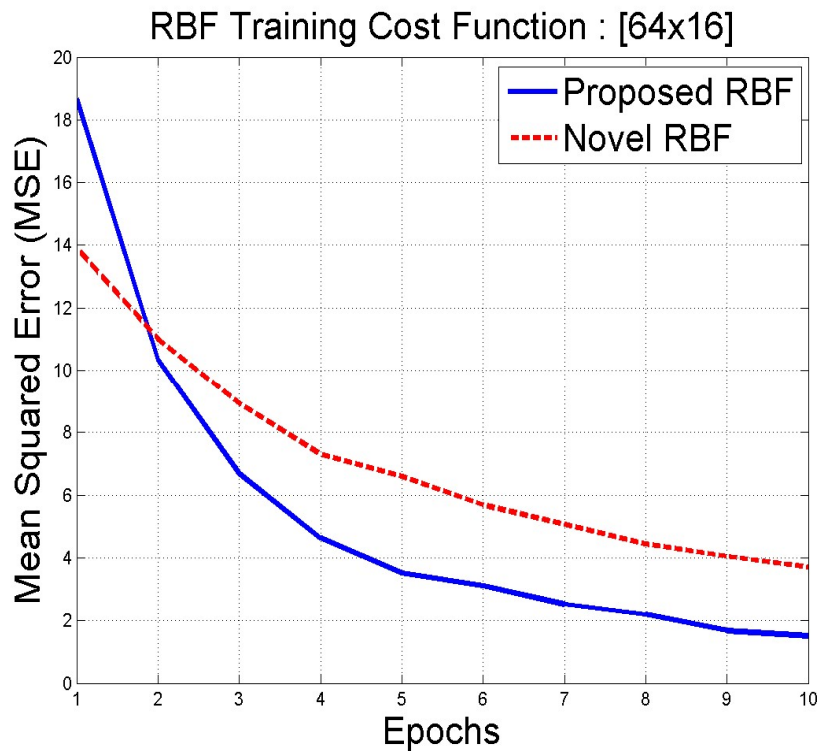


Figure 4: Training cost comparison between Novel RBF and Proposed RBF (Sequences = 64, Modulation = 16-QAM)

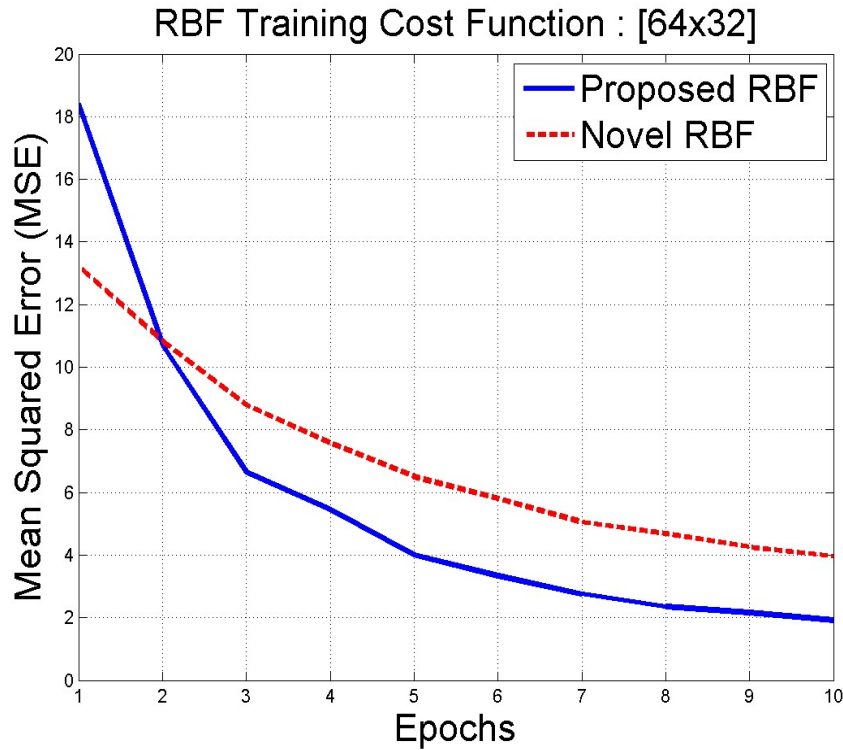


Figure 5: Training cost comparison between Novel RBF and Proposed RBF (Sequences = 64, Modulation = 32-QAM)

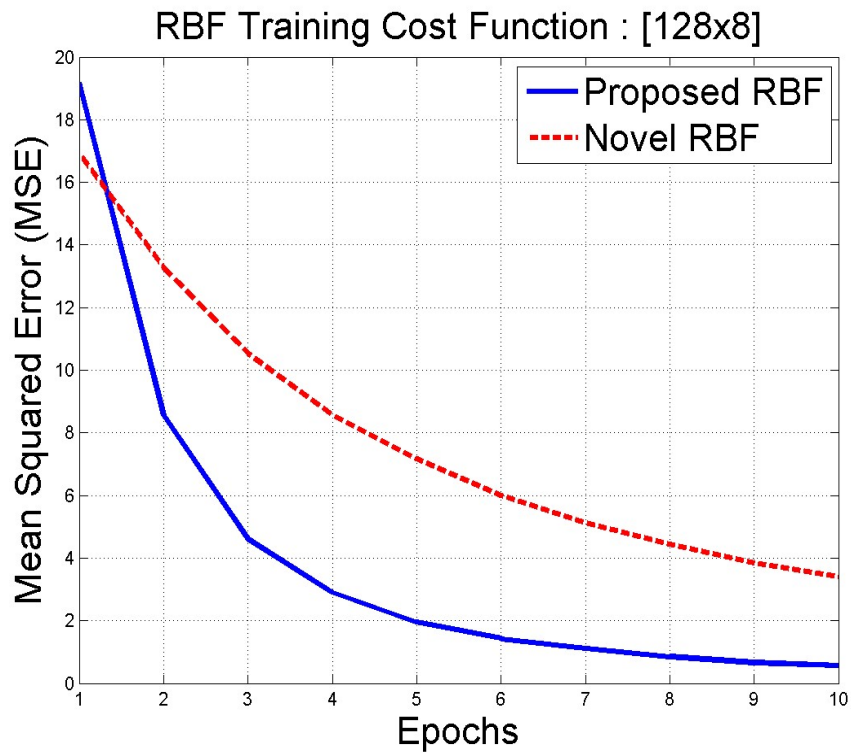


Figure 6: Training cost comparison between Novel RBF and Proposed RBF (Sequences = 128, Modulation = 8-QAM)

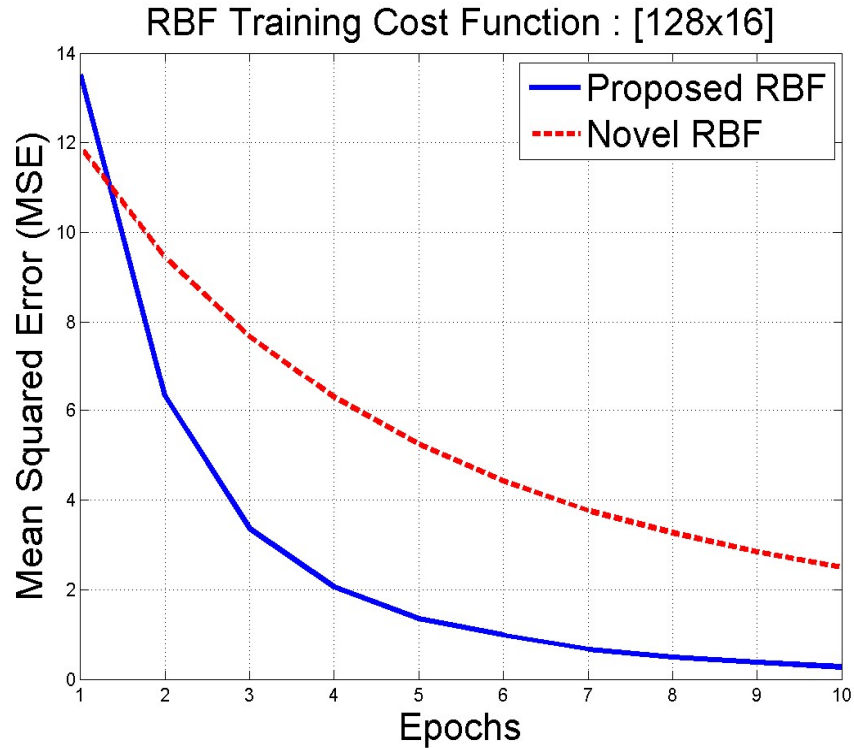


Figure 7: Training cost comparison between Novel RBF and Proposed RBF (Sequences = 128, Modulation = 16-QAM)

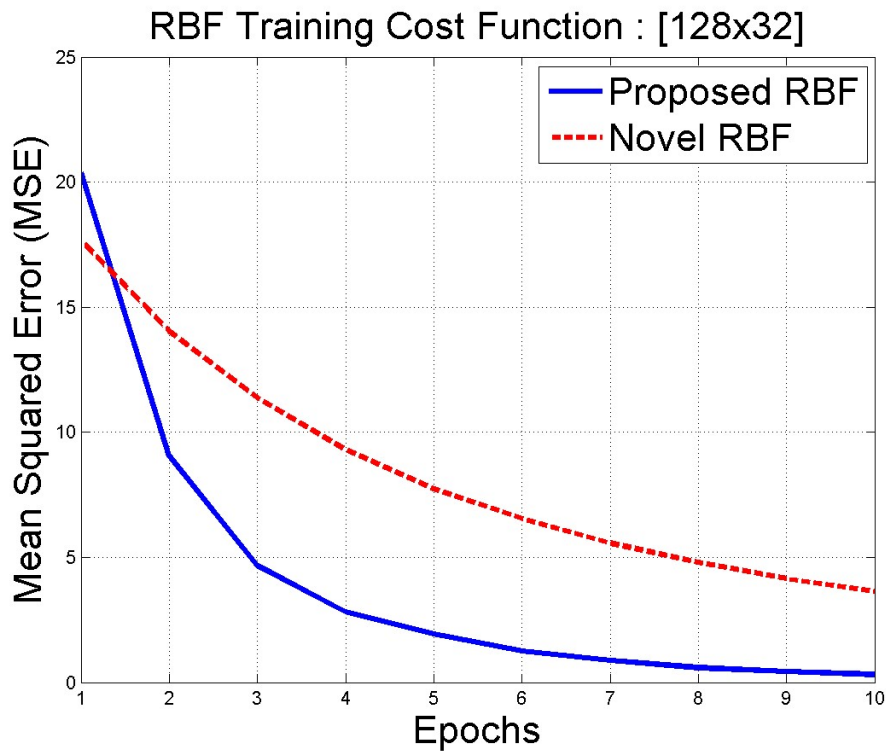


Figure 8: Training cost comparison between Novel RBF and Proposed RBF (Sequences = 128, Modulation = 32-QAM)

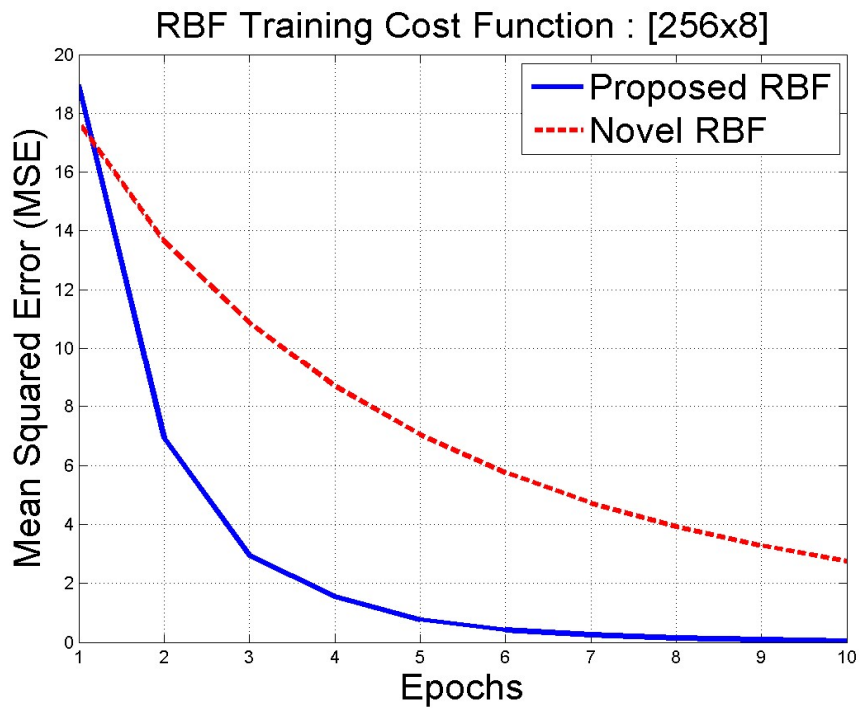


Figure 9: Training cost comparison between Novel RBF and Proposed RBF (Sequences = 256, Modulation = 8-QAM)

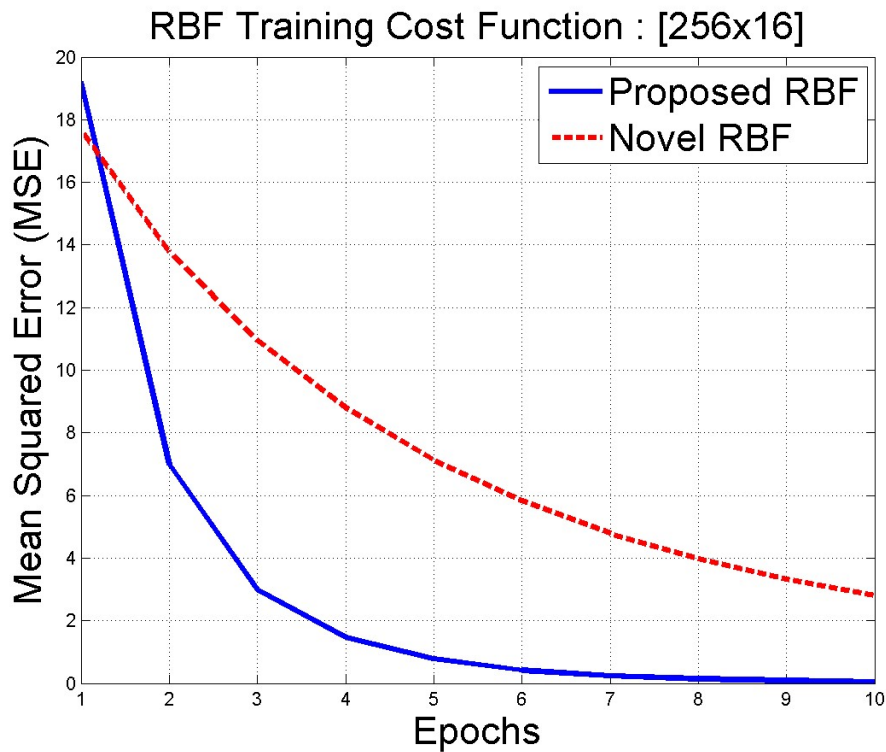


Figure 10: Training cost comparison between Novel RBF and Proposed RBF (Sequences = 256, Modulation = 16-QAM)

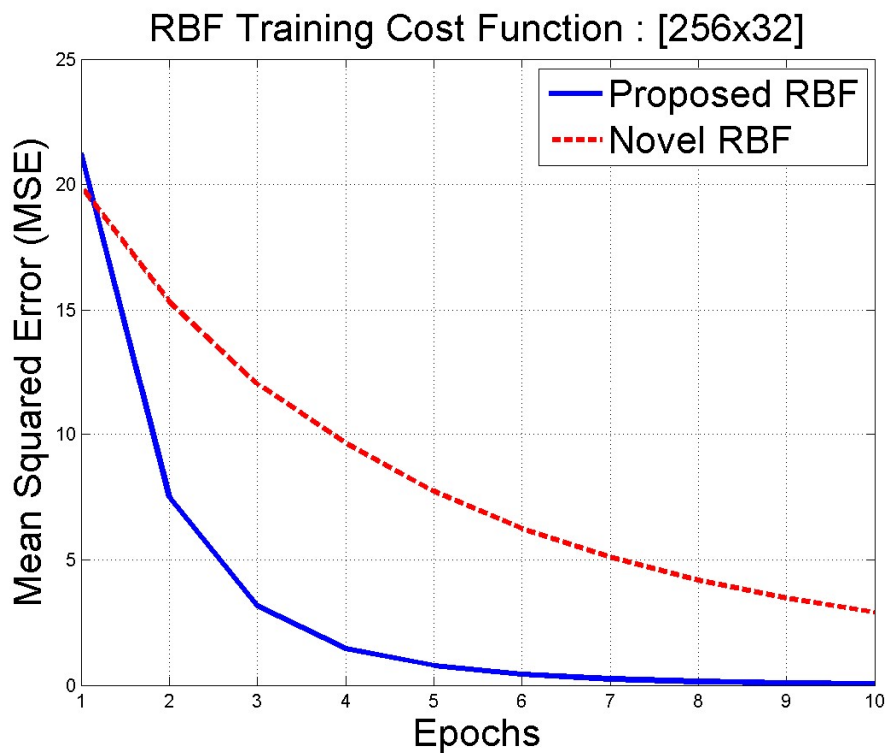


Figure 11: Training cost comparison between Novel RBF and Proposed RBF (Sequences = 256, Modulation = 32-QAM)

6.4 Testing Results

The second most important phase of performance evaluation of primarily MNKB-RBF is done and is generally termed as “Testing Phase” in the ANN community. However, in order to evaluate MNKB-RBF, we need to do its comparison with other similar algorithm. Hence, like the “Training Phase” performance of MNKB-RBF is compared with NKB-RBF and additionally with simple SLM as well.

Like the “Training Phase”, in the “Testing Phase” too three basic test cases are performed. Each testing case in turn consists of tests done on three datasets of similar nature as listed below:

Testing Case I: Dataset having 64 phase-rotated sequences.

- Dataset 1 – [64 x 8]
- Dataset 2 – [64 x 16]
- Dataset 3 – [64 x 32]

Testing Case II: 128 sequences

- Dataset 4 – [128 x 8]
- Dataset 5 – [128 x 16]

- Dataset 6 – [128 x 32]

Testing Case III: 256 sequences

- Dataset 7 – [256 x 8]
- Dataset 8 – [256 x 16]
- Dataset 9 – [256 x 32]

The results of the testing phase in graphical form are shown in Figures 12 to Figure 20. The results shown in these “Testing Case I, II and III”.

6.4.1 Evaluation, Analysis, and Deductions

The x-axis in these graphs represent the “Message Number” under focus. Recall that a total of 50 messages

are to be sent as separate transmissions selecting a phase-rotated sequence from a pool of given sequences. The sequence is to be selected in a manner to minimize PAPR for that message. Hence, it can be seen that there are 50 messages on x-axis with PAPR for each message shown on y-axis.

Each graph has three curves black solid-line curve representing our proposed RBF (MNKB-RBF), blue dashed-line curve for the Novel RBF

(NKB-RBF) and red solid-line curve for simple SLM.

At first glance it seems that the results are random. But a careful look at these graphs reveals the following.

- For majority of the messages, the red solid-line curve is below the other two curves indicating high values of PAPR for simple SLM and thus it is knocked out of the competition with NKB-RBF and MNKB-RBF.
- Comparing and carefully analyzing the solid-line black curve (MNKB-RBF) with the dashed-line blue curve (NKB-RBF) it can be seen that for majority of the messages PAPR for MNKB-RBF is lower than NKB-RBF. For only a few messages, PAPR for MNKB-RBF is higher than NKB-RBF.
- As a whole it is concluded that MNKB-RBF outperforms both Simple SLM and NKB-RBF in terms of reduction in PAPR levels.

The same pattern, i.e., curve for MNKB-RBF flowing under other curves for most of the messages, is observed in results of Test Case II & III.

6.4.2 Probability of Selecting Carrier of Low PAPR

In order to be clearer about the deduction drawn in the previous sub-section, the results of the previous sub-section are reprocessed to find the probability of selection of a phase-rotated carrier sequence with the lowest PAPR from a given pool of phase-rotated sequence. The probability is calculated for all three schemes, i.e., Simple SLM, Novel RBF, and Proposed RBF and shown in Table 4.

The 1st column of this table (from left) gives the test number. The details regarding the size of the pool of sequences and the number of symbols used for modulation are given in the 2nd column. Whereas, the 3rd, 4th, and 5th column show the probability calculated for the Simple SLM, Novel RBF, and the Proposed RBF. Please note the values in these columns give the probability of the selection of the lowest PAPR which implies that the scheme with the highest probability is the best one. Hence, for each row the highest values are underlined and produced in bold font.

One can easily notice that except for Test Case 1-3 and 3-2, the performance of the Proposed RBF is the best of the three. Therefore, we can conclude with a higher level of confidence that the performance of the Proposed RBF is better than the other two contenders.

Table 4: Probability of Selecting Carrier of Low PAPR

Test Case Number	Test Case Details (Carriers x Symbols)	SLM	Novel RBF	Proposed RBF
1-1	256 x 32	0.54	0.82	<u>0.88</u>
1-2	256 x 16	0.48	0.74	0.80
1-3	256 x 8	0.44	<u>0.80</u>	0.76
2-1	128 x 32	0.46	0.58	<u>0.60</u>
2-2	128 x 16	0.40	0.52	<u>0.66</u>
2-3	128 x 8	0.40	0.66	<u>0.68</u>
3-1	64 x 32	0.58	0.58	<u>0.62</u>
3-2	64 x 16	0.42	<u>0.60</u>	0.40
3-3	64 x 8	0.40	0.56	<u>0.58</u>

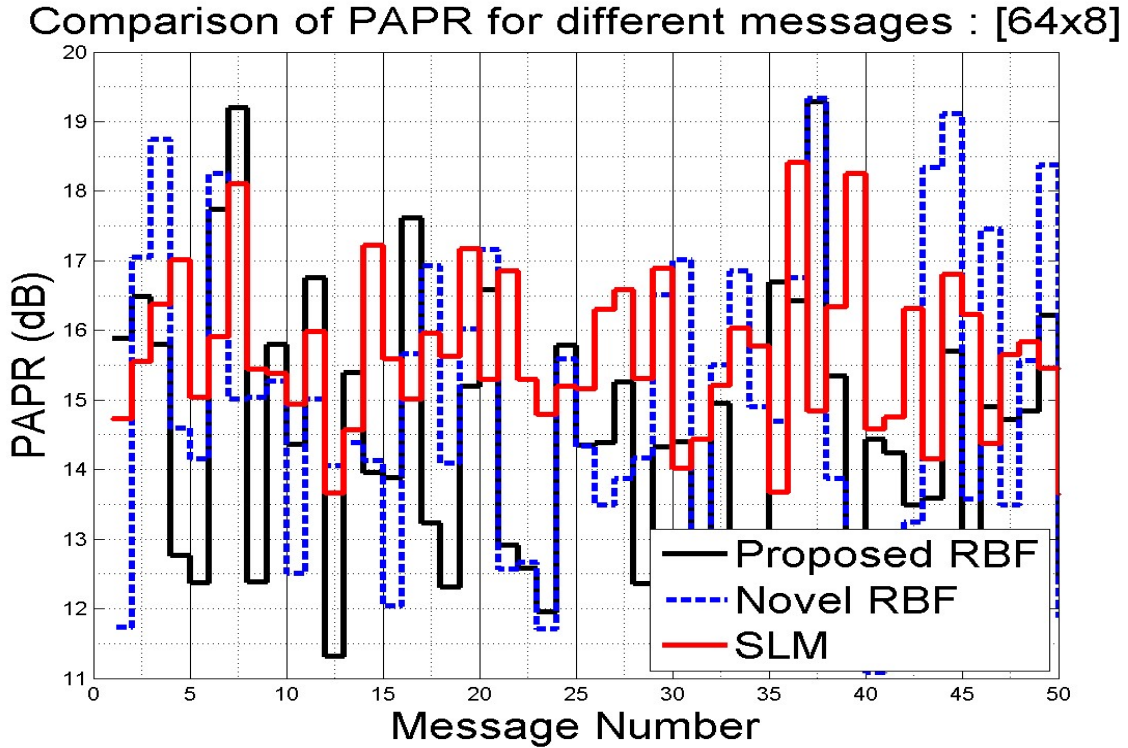


Figure 12: Sequences = 64, Modulation = 8-QAM

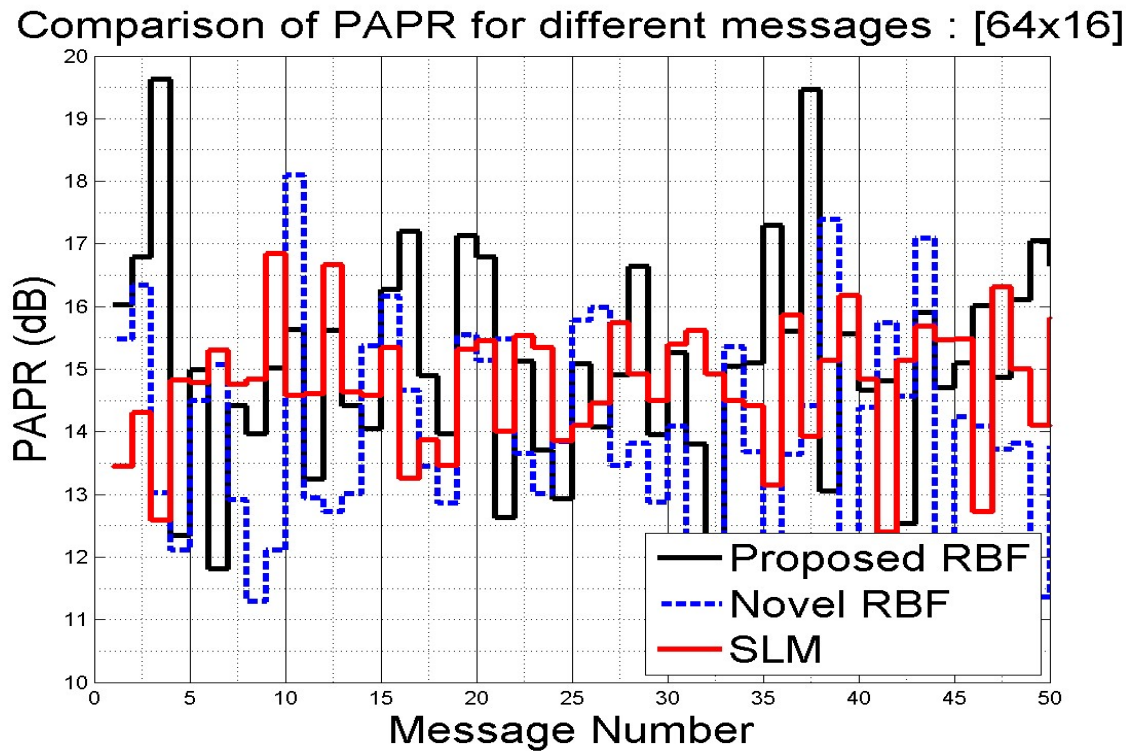


Figure 13: Sequences = 64, Modulation = 16-QAM

Comparison of PAPR for different messages : [64x32]

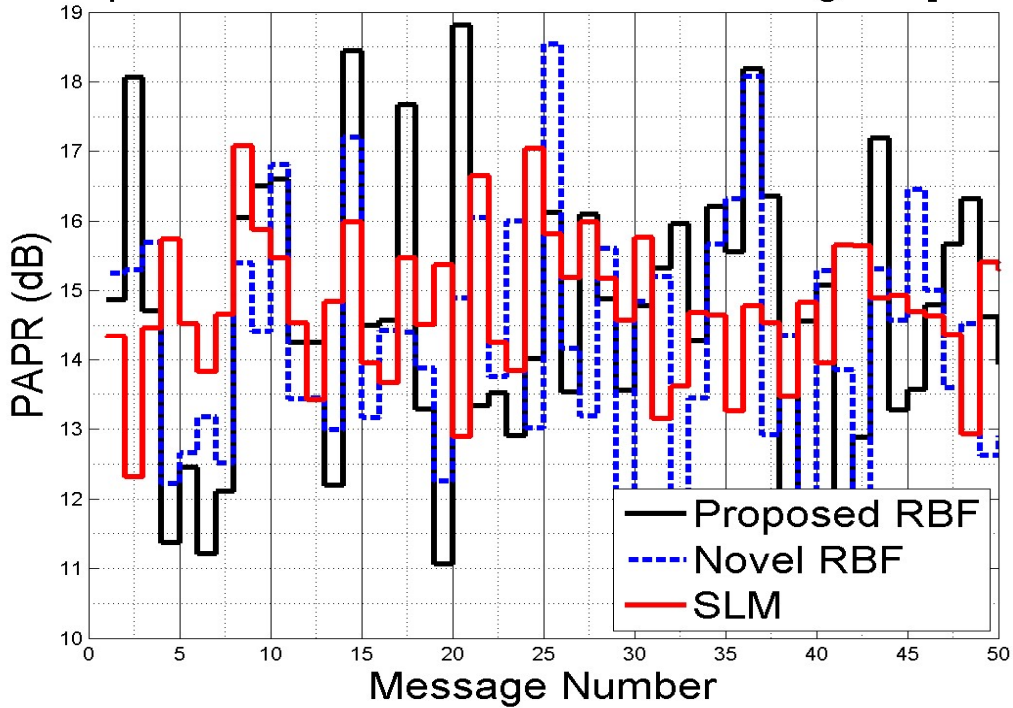


Figure 14: Sequences = 64, Modulation = 32-QAM

Comparison of PAPR for different messages : [128x8]

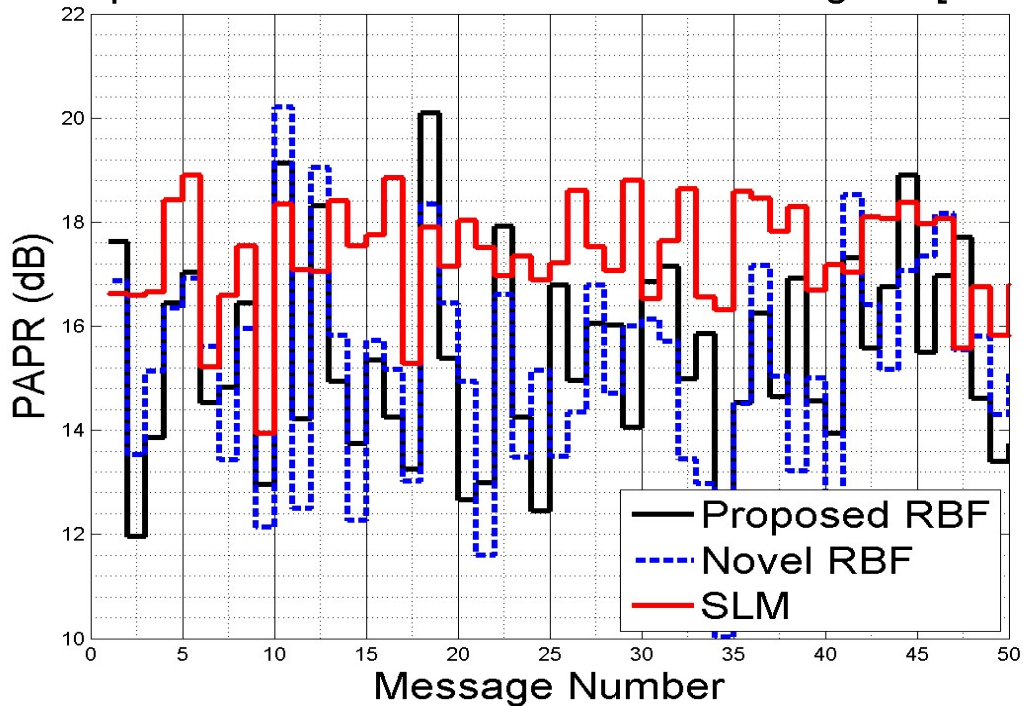


Figure 15: Sequences = 128, Modulation = 8-QAM

Comparison of PAPR for different messages : [128x16]

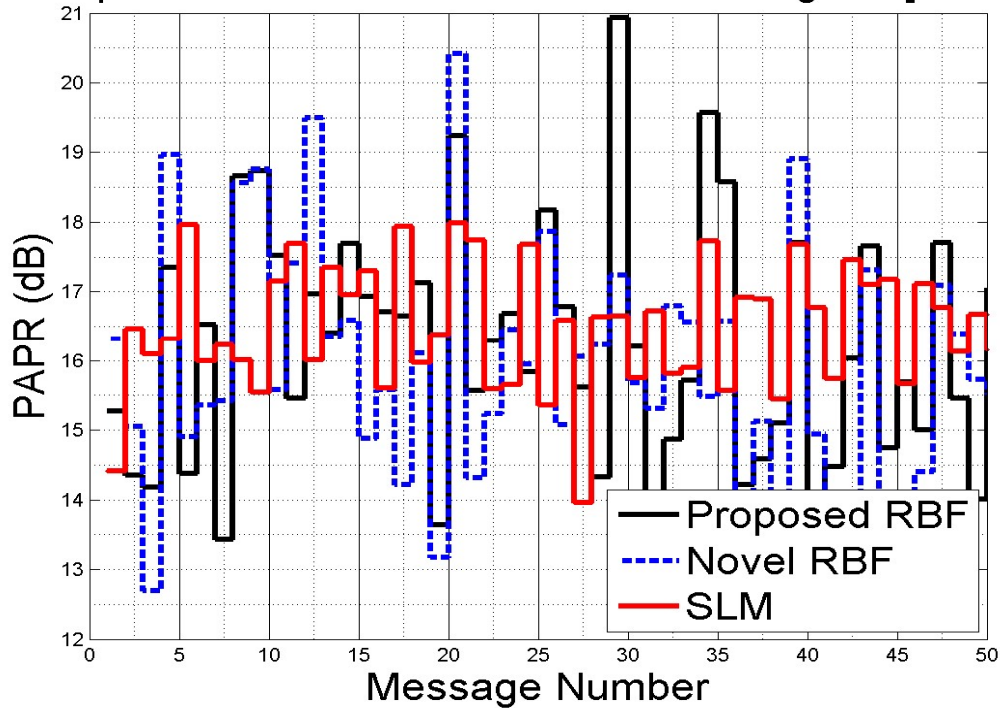


Figure 16: Sequences = 128, Modulation = 16-QAM

Comparison of PAPR for different messages : [128x32]

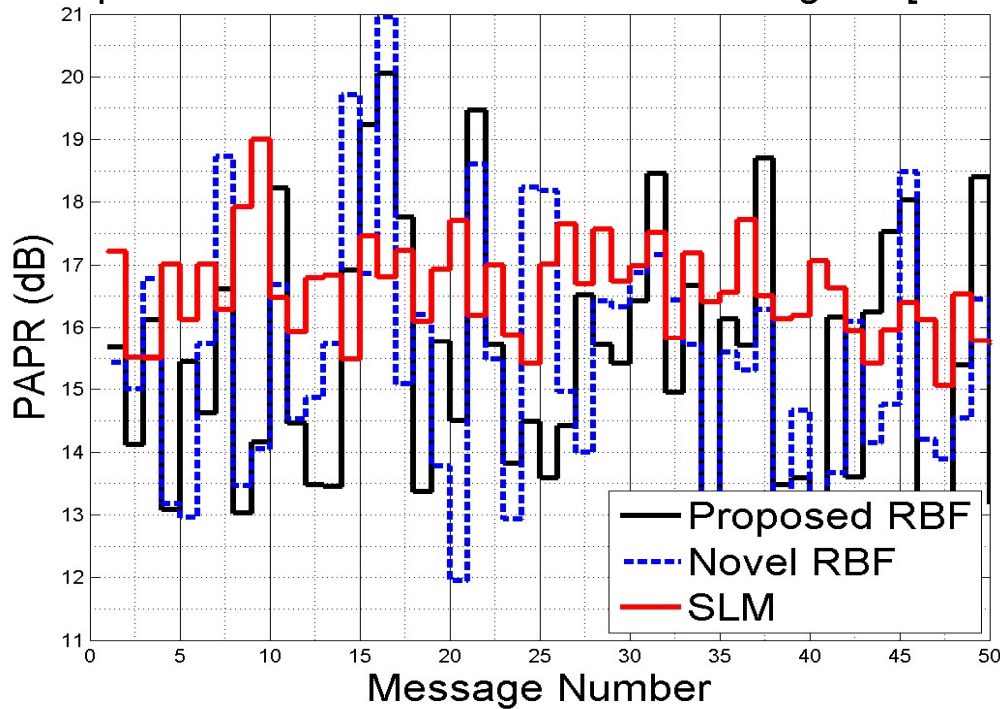


Figure 17: Sequences = 128, Modulation = 32-QAM

Comparison of PAPR for different messages : [256x8]

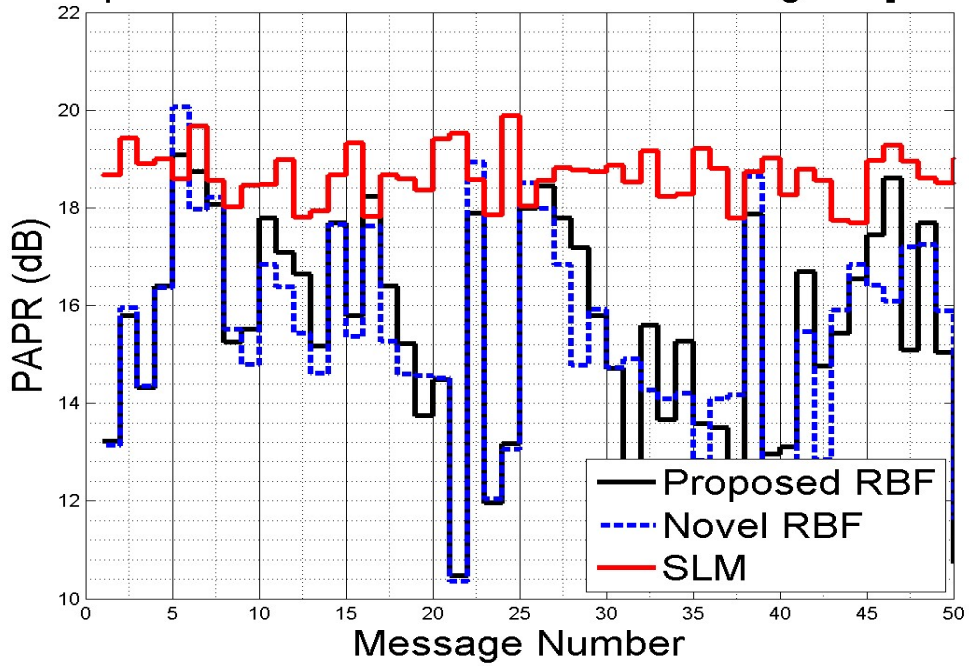


Figure 18: Sequences = 256, Modulation = 8-QAM

Comparison of PAPR for different messages : [256x16]

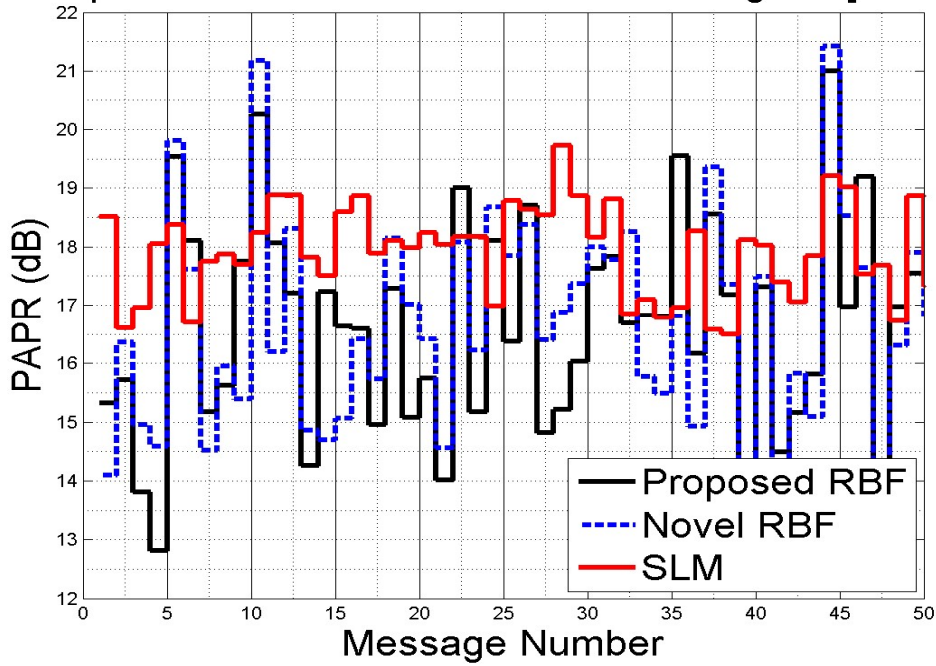


Figure 19: Sequences = 256, Modulation = 16-QAM

Comparison of PAPR for different messages : [256x32]

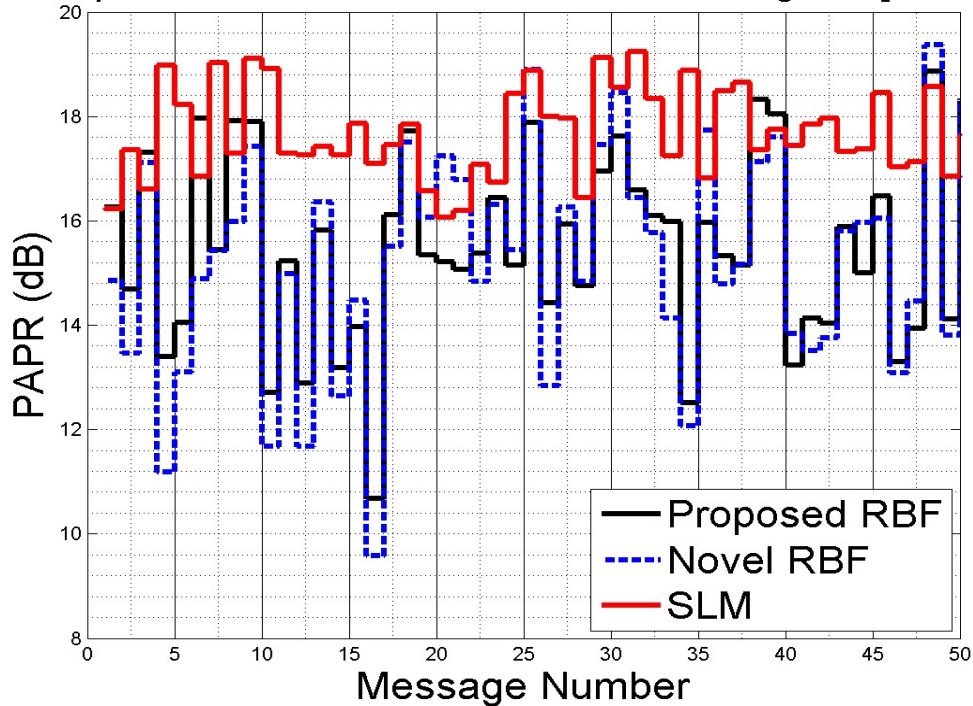


Figure 20: Sequences = 256, Modulation = 32-QAM

7 NOVELTY AND IMPACT

NKB-RBF suffers from manual selection of mixing parameters, which cause degradation in performance if optimal values are not selected, which requires prior knowledge of the system. In order to use it for optimization of selection of one phase rotated sub-sequence of signals among many candidates in SLM (with minimum PAPR), we need to make the tuning of α_1 and α_2 dynamically adaptive. The novelty of the proposed algorithm is adaptability feature which dynamically tunes mixing parameters to reach optimal values. This feature is used to minimize the overall error of the system, we also propose to use the error energy besides distance for tuning of α_1 and α_2 .

8 CONCLUSION

As stated in the previous section, the focus of this research activity is to propose a mechanism/framework which minimizes PAPR in majority of transmissions. Such a mechanism is indeed proposed and described in this dissertation. The core of the proposed scheme consists of both

SLM scheme and ANN which uses a modified version (MNKB-RBF) of already available kernel.

The conclusions of this research activity are enumerated below.

- Selective Mapping (SLM), one of the PAPR reduction schemes, has the potential for further improvement in performance and can lead to optimal selection a sequence of phase-rotated sub-carrier from a pool of available sequences such that its PAPR is the lowest.
- SLM used in conjunction with ANN has the potential to lead to optimal selection.
- A recently proposed ANN kernel (NKB-RBF) is shown to perform better but suffers from the manual selection of weights of tuning parameters α_1 and α_2 .
- The proposed kernel (MNKB-RBF) which uses error-energy to automatically adjust weights of α_1 and α_2 is shown in this dissertation through simulation results to perform better than NKB-RBF.

From analysis of simulation results (comprehensive set of scenarios) it is concluded that the probability of selection of a sequence of phase-rotated sub-carriers from a pool of given sequences

in the proposed framework is the highest among all contenders (Simple SLM, NKB-RBF based SLM).

9 FUTURE WORK

The 5G mobile networks are supposed to achieve 1000 times the system capacity, 10 times the spectral efficiency, higher data rates, 25 times the average cell throughput and other improvements over 4G systems [29]. Therefore, further improvement in existing OFDM model is still a major issue. In future work, new techniques must be investigated to increase and utilize maximum bandwidth by making OFDM more efficient for upcoming 5th generation communication systems.

REFERENCES

- [1] Chen, J., & Zhu, Z. L. (2017). "An approach for physical layer security enhancement and PAPR reduction in OFDM-PON", *Optical Fiber Technology*, 36, 370-373.
- [2] Elavarasan, P., and G. Nagarajan. "Peak-power reduction using improved partial transmit sequence in orthogonal frequency division multiplexing systems." *Computers & Electrical Engineering* 44 (2015): 80-90.
- [3] Hmood, Jassim K., Kamarul A. Noordin, Hamzah Arof, and Sulaiman W. Harun. "Peak-to-average power ratio reduction in all-optical orthogonal frequency division multiplexing system using rotated constellation approach." *Optical Fiber Technology* 25 (2015): 88-93.
- [4] Singh, Amritpal, and Harjit Singh. "Peak to average power ratio reduction in OFDM system using hybrid technique." *Optik-International Journal for Light and Electron Optics* 127, no. 6 (2016): 3368-3371.
- [5] Nagashima, T., G. Cincotti, T. Murakawa, S. Shimizu, M. Hasegawa, K. Hattori, M. Okuno et al. "Peak-to-average power ratio reduction of transmission signal of all-optical orthogonal time/frequency domain multiplexing using fractional Fourier transform." *Optics Communications* 402 (2017): 123-127.
- [6] Ochiai, Hideki. "Statistical distributions of instantaneous power and peak-to-average power ratio for single-carrier FDMA systems." *Physical Communication* 8 (2013): 47-55.
- [7] T. Jiang., and Z. Guangxi., "Complement block coding for reduction in peak-to-average power ratio of OFDM signals", *IEEE Communications Magazine*, vol. 43, no. 9, pp. S17-S22, 2005.
- [8] S. H. Muller., and J. B. Huber., "OFDM with reduced peak-to-average power ratio by optimum combination of partial transmit sequences", *Electronics Letters*, vol. 33, no. 5, pp. 368-369, February, 1997.
- [9] L. J. Cimini Jr. and N. R. Sollenberger, "Peak-to-average power ratio reduction of an OFDM signal using partial transmit sequences", *IEEE Communications Letters*, vol. 4, no. 3, pp. 86-88, March, 2000.
- [10] W. S. Ho., A. S. Madhukumar., and F. Chin., "Peak-to-average power reduction using partial transmit sequences: a suboptimal approach based on dual layered phase sequencing", *IEEE Transaction on Broadcasting*, vol. 49, no. 2, pp. 225-231, June, 2003.
- [11] Jiang. T., and Wu, Y., "An overview: Peak-to-average power ratio reduction techniques for OFDM signals", *IEEE Transaction On Broadcasting*, vol. 54, no. 2, pp. 257-268, June, 2008.
- [12] Farzana Abro, Manzoor Hashmani, A. N. Khizer, Mukhtiar Unar, "Performance Analysis of Selected Mapping Scheme for Minimization of Peak to Average Power Ratio in OFDM Systems", *Sindh University Research Journal (Science Series) Pakistan*, Vol.47, No.3, pp. 419-424, August 2015.
- [13] Bauml, R.W., Fischer, R.F.H., and Huber, J.B. "Reducing the peak to average power ratio of multi carrier modulation by selective mapping", *IEEE Electronics Letters*, vol. 32, no. 22, pp. 2056-2057, October, 1996.
- [14] Kumari, Nutan, and Simarpreet Kaur. "A Survey on Various PAPR Reduction Techniques in OFDM Communication Systems." *International Research Journal of Engineering and Technology (IRJET)* 2.06 (2015)
- [15] Kumari, Shailly, and Rajesh Mehra. "Selective Mapping and Partial Transmit Sequence Based PAPR Reduction for OFDM Applications." *IOSR Journal of VLSI and Signal Processing* 6.6 (2016): 70-76.
- [16] W. S. McCulloch and W. Pitts "A logical calculus of the ideas immanent in nervous activity" *The Bulletin of Mathematical Biophysics*, vol. 5, no. 4, pp. 115-133, 1943.

- [17] J. Khan, J. S. Wei., M. Ringer et al., "Classification and diagnostic prediction of cancers using gene expression profiling and artificial neural networks," *Nature Medicine*, vol. 7, no. 6, pp.673–679, 2001.
- [18] G. Zhang, B. E. Patuwo, and M. Y. Hu, "Forecasting with artificial neural networks: the state of the art," *International Journal of Forecasting*, vol. 14, no. 1, pp. 35–62, 1998.
- [19] Onder, Mursel, and Aydin Akan. "Pilot tone investigation for joint channel estimation, equalization, and demodulation based on neural networks." *Electrical and Electronics Engineering (ELECO), 2015 9th International Conference on*. IEEE, 2015.
- [20] Ahmad, Syed Tajammul, and K. Pradeep Kumar. "Radial basis function neural network nonlinear equalizer for 16-QAM coherent optical OFDM." *IEEE Photonics Technology Letters* 28.22 (2016): 2507-2510.
- [21] D. S. Broomhead., and D. Lowe., "Multivariable functional interpolation and adaptive networks", *Complex Systems*, vol. 2, no. 3, pp. 321–355, 1988.
- [22] J. Park and I. W. Sandberg, "Universal Approximation using Radial Basis Function Networks", *Neural Computation*, vol. 3, no. 2, pp. 246–257, 1991.
- [23] H. Leung, T. Lo, and S. Wang, "Prediction of noisy chaotic time series using an optimal radial basis function neural network," *IEEE Transactions on Neural Networks*, vol. 12, no. 5, pp. 1163–1172, 2001.
- [24] S. Seshagiri and H. K. Khalil, "Output feedback control of nonlinear systems using RBF neural networks," *IEEE Transactions on Neural Networks*, vol. 11, no. 1, pp. 69–79, 2000.
- [25] J. Platt, "A resource-allocating network for function interpolation," *Neural Computation*, vol. 3, no. 2, pp. 213–225, 1991.
- [26] D. Wettschereck., and T. Dietterich., "Improving the performance of radial basis function networks by learning center locations", *Advances in Neural Information Processing Systems*, vol. 4, no. 1, pp. 1133-1140, Morgan Kaufmann, San Mateo, Calif, USA, 1992.
- [27] Aftab, W., Moinuddin, M., and Shaikh, M. S., "A Novel Kernel for RBF Based Neural Networks", *Abstract and Applied Analysis*, vol. 01, no. 04, pp. 222-555, June, 2014. Article ID 176253, Hindawi Publishing Corporation.
- [28] T. Aboulnasr., and K. Mayyas., "A Robust Variable Step-Size LMS type Algorithm: Analysis and Simulation," *IEEE Transactions on Signal Processing*, vol. 45, no. 3, pp. 631–639, 1997.
- [29] Sandoval, Francisco, Gwenael Poitau, and François Gagnon. "Hybrid Peak-to-Average Power Ratio Reduction Techniques: Review and Performance Comparison." *IEEE Access* 5 (2017): 27145-27161.